International Journal of Innovative Computing, Information and Control
Volume **16**, Number **2**, April **2020**

ICIC International ©2020 ISSN 1349-4198
pp. 733–748

FIXED-TIME DYNAMIC SURFACE CONTROL FOR POWER SYSTEMS WITH STATCOM

Adirak Kanchanaharuthai[1] and Ekkachai Mujjalinvimut[2]

[1]Department of Electrical Engineering
Rangsit University
52/347 Muang-Ake, Phaholyothin Road, Lak-Hok, Muang, Patumthai 12000, Thailand
adirak@rsu.ac.th

[2]Department of Electrical Engineering
Faculty of Engineering
King Mongkut's University of Technology Thonburi
Pracha Uthit Road, Bang Mod, Bangkok 10140, Thailand
ekkachai.muj@kmutt.ac.th

Received September 2019; revised January 2020

Abstract. *This paper develops a fixed-time control design for power systems with STATCOM via a dynamic surface control approach. In order to avoid the problem of "explosion of terms" inherent in backstepping algorithm, the proposed dynamic surface control strategy is developed to avoid such a problem. Based on the Lyapunov direct method, the stability of the closed-loop dynamics is proved to ensure that all trajectories of the closed-loop dynamics are semi-globally fixed-timely uniformly ultimately bounded. The effectiveness and superiority of the presented design are verified on a single-machine infinite bus power system. The simulation results exhibit that the presented control can effectively improve dynamic performances, rapidly suppress power system oscillations of the overall closed-loop dynamics in a fixed time, and has the superior performances over a conventional dynamic surface control approach.*

Keywords: Dynamic surface control, Fixed-time stability, STATCOM, Generator excitation

1. **Introduction.** There is a rapidly increasing growth in the size and complexity of modern power systems. Therefore, such power systems are highly nonlinear complex dynamical systems, thereby leading difficulties to maintain power system stability and operation. With a complex nonlinear dynamic behavior of power systems, there are lots of attempts in finding out effective and promising methods to enhance system stability and dynamic performances under unpredictable disturbances. To enhance power system stability and achieve the desired control objectives, there are recently major three approaches: an excitation control of synchronous generators [1], a combined generator excitation with energy storage system control [2], and a combination of generator excitation and Flexible AC Transmission System (FACTS) devices [3, 4].

Because of currently fast developments in power electronic devices, the combined generator excitation control and FACTS devices provide an opportunity to effectively deal with a variety of problems such as the existing transmission facilities and several constraints to build new transmission lines. Among FACTS family, Static Synchronous Compensator (STATCOM) [3, 4] is used in this paper to increase the grid transfer capability, improve voltage stability, damp out power oscillation, and enhance transient stability. Moreover,

DOI: 10.24507/ijicic.16.02.733

to further cope with several problems arising in power systems, the coordination of generator excitation and STATCOM is a promising and effective approach and has received increasing attention.

To the best of our knowledge, a variety of control design techniques for a combined generator excitation and STATCOM control [5-15] via nonlinear control theory have been investigated. A nonlinear feedback linearizing controller [5] based on a coordination of the zero dynamic approach and the pole-assignment method was presented for transient stability enhancement of Single-Machine Infinite Bus (SMIB) system. A coordinated adaptive nonlinear control was developed to improve power system stability of a Single-Machine Infinite Bus system (SMIB) [6] and multi-machine power systems [7, 8]. Using backstepping design combined with passivity theory, a coordinated nonlinear control [9] was designed. An interconnection and damping assignment passivity-based control [10] was proposed to improve both transient stability and voltage regulation. Based on Immersion and Invariance (I&I) design [11], a nonlinear control was presented for the power systems in the presence of unknown parameters. An intelligent control design [12] was proposed for dealing with random loads in both SMIB and large-scale power systems. Kanchanaharuthai and Mujjalinvimut [13] proposed a backstepping control with rapid-convergent differentiator to avoid the problem of "explosion of complexity" [14] arising in calculating the derivative of the virtual control functions. The rapid-convergent differentiator design is used to estimate the derivative of the virtual control functions, and has a high precision together with no chattering behavior. More recently, Ni et al. [15] proposed a nonlinear controller via a combination of Dynamic Surface Control (DSC) [16], high-order sliding mode control, and fixed-time stability theory to address voltage stabilization, to suppress chaotic oscillation in power systems with current source converter-based STATCOM, and to accomplish good chaos suppression performances.

Motivated by these control methods, this paper continues this line of investigation but uses a new control design to avoid the problem of "explosion of terms". This problem often occurs in large-scale systems, thereby leading to a complexity from computing the derivative of the virtual control functions in each design step. There have recently been three methods employed to cope with this problem. The first one is a command filtered backstepping method [17] which can be viewed as another modified backstepping control. This method introduces a command filter that avoids analytic computation of derivatives of virtual control functions but approximates the derivative of the virtual control instead. The errors from the command filters can be reduced with the combination of compensation signals. The second one is a first-order Levant differentiator [18] that can exactly estimate the derivatives in finite time. However, this technique has an unavoidable drawback because the parameters of first differentiator need to be suitably selected. The last one is a dynamic surface control method using dynamic linear filters to avoid directly computing the derivatives of virtual control functions. However, this paper introduces nonlinear filters to find out the derivatives of such virtual control functions. Following an idea given in [15], the nonlinear filters used in the design procedure of this paper not only further improve transient performances, but also help drive all trajectories of the closed-loop system to the desired equilibrium in a fixed time.

In this paper, a systematic control algorithm for designing a nonlinear stabilizing feedback controller for power systems with STATCOM via a dynamic surface control is presented. In addition, with the help of a combination of DSC approach and the fixed-time control design, the proposed control scheme can accomplish semi-global uniformly ultimate boundedness of all trajectories of the system within finite time. Although the developed control design follows the idea presented in [15], the main differences are as follows: (i) the presented control focuses on the design of a state feedback control law

using different measurable states such as active power of excitation and STATCOM; (ii) enhancement of transient stability and voltage regulation together with faster response ability are stressed.

Therefore, the major contributions of this paper are summarized as follows: (i) A fixed-time stable dynamic surface control scheme which can improve transient stability and stabilize the power systems with STATCOM, has not been investigated before; (ii) All trajectories of the overall closed-loop system are semi-globally ultimately bounded and converge to a small neighborhood of the equilibrium point within a fixed time; and (iii) Compared with a conventional dynamic surface control, the presented controller without computing directly the virtual control functions offers more advantages: faster response ability and the shorter settling time to reach the desired equilibrium, further enhancement of power system stability.

The rest of this paper is organized as follows. Simplified synchronous generator and STATCOM models are briefly described and control problem formulation is given in Section 2. A fixed-time DSC design is given in Section 3. Simulation results are given in Section 4. Conclusions are given in Section 5.

2. Power System Model Description.

2.1. Power system models with STATCOM. The complete dynamical model [6, 11] of the synchronous generator connected to an infinite bus with STATCOM dynamics can be expressed as follows:

$$\begin{cases} \dot{\delta} = \omega - \omega_s \\ \dot{\omega} = \dfrac{1}{M}\left(P_m - P_e - P_s - D(\omega - \omega_s)\right) \\ \dot{P}_e = (-a + \cot\delta(\omega - \omega_s))P_e + \dfrac{bV_\infty \sin 2\delta}{2(X_1 + X_2)} + \dfrac{V_\infty \sin\delta}{(X_1 + X_2)} \cdot \dfrac{u_f}{T_0'} \\ \dot{P}_s = \mathcal{N}(\delta, P_e, P_s)(-a + \cot\delta(\omega - \omega_s))P_e + \dfrac{\mathcal{N}(\delta, P_e, P_s) bV_\infty \sin 2\delta}{2(X_1 + X_2)} \\ \qquad + \dfrac{\mathcal{N}(\delta, P_e, P_s)V_\infty \sin\delta}{(X_1 + X_2)} \cdot \dfrac{u_f}{T_0'} + \dfrac{P_e X_1 X_2}{\Delta(\delta, P_e)} \cdot \dfrac{1}{T}\left(-\left(\dfrac{P_s \Delta(\delta, P_e)}{P_e X_1 X_2} - I_{qe}\right) + u_q\right) \end{cases} \tag{1}$$

with

$$\Delta(\delta, P_e) = \sqrt{\left(\frac{P_e(X_1 + X_2)X_2}{V_\infty \sin\delta}\right)^2 + (V_\infty X_1)^2 + 2X_1 X_2 P_e (X_1 + X_2)\cot\delta},$$

$$\mathcal{N}(\delta, P_e, P_s) = \frac{P_s}{P_e} - \frac{P_s}{\Delta(\delta, P_e)^2}\left(X_1 X_2 \cot\delta(X_1 + X_2) + P_e\left(\frac{X_2(X_1 + X_2)}{V_\infty \sin\delta}\right)^2\right),$$

$$P_e = \frac{EV_\infty \sin\delta}{(X_1 + X_2)}, \quad P_s = \frac{P_e I_Q X_1 X_2}{\Delta(\delta, E)}, \quad I_Q = \frac{P_s \Delta(\delta, P_e)}{P_e X_1 X_2},$$

where δ is the power angle of the generator, ω denotes the relative speed of the generator, $D \geq 0$ is a damping constant, P_m is the mechanical input power, E denotes the generator transient voltage source, $P_E = \frac{EV_\infty \sin\delta}{X_{d\Sigma'}}$ is the electrical power, without STATCOM, delivered by the generator to the voltage at the infinite bus V_∞, ω_s is the synchronous machine speed, $\omega_s = 2\pi f$, H represents the per unit inertial constant, f is the system frequency and $M = 2H/\omega_s$. $X'_{d\Sigma} = X'_d + X_T + X_L$ is the reactance consisting of the direct axis transient reactance of SG, the reactance of the transformer, and the reactance of the transmission line X_L. Similarly, $X_{d\Sigma} = X_d + X_T + X_L$ is identical to $X'_{d\Sigma}$ except

that X_d denotes the direct axis reactance of synchronous generators. T_0' is the direct axis transient short-circuit time constant. u_f is the field voltage control input to be designed. I_Q denotes the injected or absorbed STATCOM currents as a controllable current source, I_{Qe} is an equilibrium point of STATCOM currents, u_q is the STATCOM control input to be designed, and T is a time constant of STATCOM models.

For convenience, let us introduce new state variables as follows:

$$x_1 = \delta - \delta_e, \quad x_2 = \omega - \omega_s, \quad x_3 = P_e, \quad x_4 = P_s \tag{2}$$

Subsequently, after differentiating the state variables (2), we have the power system with STATCOM which can be written in the following form of an affine nonlinear system[1]:

$$\dot{x} = f(x) + g(x)u(x) \tag{3}$$

where

$$\begin{cases} f(x) = \begin{bmatrix} f_1(x) \\ f_2(x) \\ f_3(x) \\ f_4(x) \end{bmatrix} = \begin{bmatrix} x_2 \\ \frac{1}{M}\left(P_m - x_3 - x_4 - Dx_2\right) \\ (-a + x_2 \cot x_1)x_3 + \frac{bV_\infty \sin 2x_1}{2(X_1+X_2)} \\ \mathcal{N}(-a + x_2 \cot x_1)x_3 + \frac{\mathcal{N}bV_\infty \sin 2x_1}{2(X_1+X_2)} - \frac{x_3 X_1 X_2 \left(\frac{x_4 \Delta(x_1,x_3)}{x_3 X_1 X_2} - I_{qe}\right)}{\Delta(x_1,x_3)} \end{bmatrix} \\ g(x) = \begin{bmatrix} 0 & 0 \\ 0 & 0 \\ g_{31}(x) & 0 \\ g_{41}(x) & g_{42}(x) \end{bmatrix} = \begin{bmatrix} 0 & 0 \\ 0 & 0 \\ \frac{V_\infty \sin x_1}{(X_1+X_2)} & 0 \\ \frac{\mathcal{N}V_\infty \sin x_1}{(X_1+X_2)} & \frac{x_3 X_1 X_2}{\Delta(x_1,x_3)} \end{bmatrix}, \; x = \begin{bmatrix} x_1 \\ x_2 \\ x_3 \\ x_4 \end{bmatrix}, \; u(x) = \begin{bmatrix} \frac{u_f}{T_0'} \\ \frac{u_q}{T} \end{bmatrix} \end{cases} \tag{4}$$

The region of operation is defined in the set $\mathcal{D} = \left\{ x \in \mathcal{S} \times \mathbb{R} \times \mathbb{R} \times \mathbb{R} \times \mathbb{R} \middle| \; 0 < x_1 < \frac{\pi}{2} \right\}$. The open loop operating equilibrium is denoted by $x_e = [0,\ 0,\ x_{3e},\ x_{4e}]^T = [0,\ 0,\ P_m,\ 0]^T$.

For the sake of simplicity, the power system considering (3) and (4) can be expressed as follows.

$$\begin{cases} \dot{x}_1 = x_2 \\ \dot{x}_2 = \dfrac{1}{M}\left(P_m - x_3 - x_4 - Dx_2\right) \\ \dot{x}_3 = f_3(x) + g_{31}(x)\dfrac{u_f}{T_0'} \\ \dot{x}_4 = f_4(x) + g_{41}(x)\dfrac{u_f}{T_0'} + g_{42}(x)\dfrac{u_q}{T} \end{cases} \tag{5}$$

2.2. **Preliminaries.**

Definition 2.1. [15] *Consider the following dynamical system:*

$$\dot{x}(t) = f(x(t)), \quad x(0) = x_0 \tag{6}$$

The trajectory of the system (6) is said to be Semi-Globally Fixed-Timely Uniformly Ultimately Bounded (SGFTUUB) if there exists a bounded function T: $R^n \to R^+$ independent of x_0, a given compact set $W_0 \in R^n$ and an arbitrarily small compact set $W \subset R^n$ which contains the origin as an interior point, such that all trajectories starting from the set W_0, they will enter the set W in finite time t_f upper bounded by T, and remain in it thereafter, i.e., $\|x(t)\| \in W$ for all $t \geq t_f$ and $\lim_{x_0 \to +\infty} t_f \leq T$ holds.

[1]It is assumed that throughout this paper all functions and mappings are $\mathbb{C}^\infty$.

Lemma 2.1. [15] *For a dynamical system $\dot{x}(t) = f(t, x)$, $x(0) = x_0$, where $x \in R^n$ and f: $R_+ \times R^n \to R^n$, and suppose the origin is an equilibrium point. If there exists a C^1 function $V(x)$: $U \to R$ such that (i) $V(x)$ is positive definite; (ii) There exist positive real numbers $\bar{\alpha}$ and $\bar{\beta}$, and an arbitrarily small positive real number ς, positive odd integers $\bar{m}$, $\bar{n}$, $\bar{p}$, $\bar{q}$ that satisfy $\bar{m} > \bar{n}$, $\bar{p} < \bar{q}$ and a compact set W_0 such that $\dot{V} \le -\bar{\alpha}V^{\bar{m}/\bar{n}} - \bar{\beta}V^{\bar{p}/\bar{q}} + \varsigma$, $x_0 \in W_0$, then the system is SGFTUUB and the system can be stabilized to arbitrarily small neighbor of the origin, i.e., $V(x) \le 2\gamma_1$ with $\bar{\alpha}\gamma_1^{\bar{m}/\bar{n}} + \bar{\beta}\gamma_1^{\bar{p}/\bar{q}} = \varsigma$, within finite time upper bounded by*

$$T_f \le T_{\max} = \frac{1}{\bar{\alpha}} \frac{\bar{n}}{\bar{m} - \bar{n}} + \frac{1}{\bar{\beta}\left(2^{\bar{p}/\bar{q}} - 1\right)} \frac{\bar{q}}{\bar{q} - \bar{p}} \tag{7}$$

Lemma 2.2. [15] *For every positive real a, b, c and positive real p, q satisfying $1/p + 1/q = 1$, the following inequality holds:*

$$ab \le c^p \frac{a^p}{p} + c^{-q} \frac{b^q}{q} \tag{8}$$

Lemma 2.3. [20] *For any nonnegative real numbers $\xi_1, \xi_2, \ldots, \xi_n$ and $0 < p \le 1$, the following inequality holds:*

$$\sum_{i=1}^{n} \xi_i^p \ge \left(\sum_{i=1}^{n} \xi_i \right)^p \tag{9}$$

Lemma 2.4. [20] *For any nonnegative real number $\xi_1, \xi_2, \ldots, \xi_n$ and $p > 1$, the following inequality holds:*

$$\sum_{i=1}^{n} \xi_1^p \ge n^{1-p} \left(\sum_{i=1}^{n} \xi_i \right)^p \tag{10}$$

Lemma 2.5. [21] *For $x, y \in R^+$ and $p \ge 1$, the following inequality holds:*

$$(x - y)^p \le x^p - y^p \tag{11}$$

Control Problem Formulation: The aim of this paper is to solve the control problem of the fixed-time stabilization of the power systems with STATCOM (5). We can formulate the control problem as follows. For the system (5), with the help of the dynamic surface control design, find out, if possible, a fixed-time controller $u(x)$ such that all trajectories of the overall closed-loop dynamics are semi-globally uniformly ultimately bounded within a fixed time independent of initial conditions. In addition, we are able to adjust arbitrarily the system convergence time by selecting controller parameters.

3. **Fixed-Time DSC Control Design and Stability Analysis.** In this section, the fixed-time dynamic surface control law for stabilizing the power systems with STATCOM is designed. The proposed design procedure can be divided into two parts. The first part is to develop a state feedback fixed-time control algorithm with the help of the dynamic surface control method. In the second part, the overall closed-loop power system stability with the help of Lyapunov stability arguments is investigated so that the obtained control law can accomplish both fixed-time control and the system performance.

3.1. **Fixed-time DSC control design.** The proposed control procedure is developed step by step as follows.

Step 1: First, we focus on the first subsystem (5), and then let us define the error surface $S_1 = x_1$. In order to accomplish fixed-time stability for the error surface S_1, differentiating S_1 with respect to time yields

$$\dot{S}_1 = x_2 \tag{12}$$

From (12), we assume x_2 as a virtual control input; thus, the desired feedback control x_2^* is able to be designed as

$$x_2^* = -\alpha_1|S_1|^{\frac{m}{n}}\text{sign}(S_1) - \beta_1|S_1|^{\frac{n}{m}}\text{sign}(S_1) \tag{13}$$

where α_1 and β_1 are positive design constants. Introduce a new state variable x_{2d} and let x_2^* pass through a first-order filter with time constant τ_2 to obtain the dynamics of x_{2d} as follows:

$$\begin{aligned} &\tau_2\dot{x}_{2d} + x_{2d} = -|x_{2d} - x_2^*|^{\frac{m}{n}}\text{sign}(x_{2d} - x_2^*) - |x_{2d} - x_2^*|^{\frac{n}{m}}\text{sign}(x_{2d} - x_2^*) \\ &x_{2d}(0) = x_2^*(0) \end{aligned} \tag{14}$$

Step 2: Define the second surface as

$$S_2 = x_2 - x_{2d} \tag{15}$$

Then, by calculating the derivative of (15), we have

$$\dot{S}_2 = \frac{1}{M}\left(P_m - x_3 - x_4 - Dx_2\right) - \dot{x}_{2d} = -\alpha_2|S_2|^{\frac{m}{n}}\text{sign}(S_2) - \beta_2|S_2|^{\frac{n}{m}}\text{sign}(S_2) \tag{16}$$

where α_2 and β_2 are positive design constants. Similarly, assuming x_3 and x_4 as the virtual control laws so the desired feedback control variables x_3^* and x_4^* can be chosen as follows:

$$x_3^* = P_m - \frac{D}{2}x_2 + \frac{M}{2}\left(\alpha_2|S_2|^{\frac{m}{n}}\text{sign}(S_2) + \beta_2|S_2|^{\frac{n}{m}}\text{sign}(S_2) - \dot{x}_{2d}\right), \quad x_4^* = x_3^* - P_m \tag{17}$$

where $\dot{x}_{2d}$ can be directly computed from (14).

Similarly, we introduce two new state variables x_{3d} and x_{4d}, and let x_3^* and x_4^* pass through a first-order filter with time constants τ_3, τ_4 together with the dynamics of both new state variables as

$$\begin{aligned} &\tau_3\dot{x}_{3d} + x_{3d} = -|x_{3d} - x_3^*|^{\frac{m}{n}}\text{sign}(x_{3d} - x_3^*) - |x_{3d} - x_3^*|^{\frac{n}{m}}\text{sign}(x_{3d} - x_3^*) \\ &x_{3d}(0) = x_3^*(0) \end{aligned} \tag{18}$$

$$\begin{aligned} &\tau_4\dot{x}_{4d} + x_{4d} = -\,|x_{4d} - x_4^*|^{\frac{m}{n}}\,\text{sign}(x_{4d} - x_4^*) - |x_{4d} - x_4^*|^{\frac{n}{m}}\text{sign}(x_{4d} - x_4^*) \\ &x_{4d}(0) = x_4^*(0) \end{aligned} \tag{19}$$

Step 3: Finally, define the third and the fourth surfaces as follows:

$$S_3 = x_3 - x_{3d}, \quad S_4 = x_4 - x_{4d} \tag{20}$$

Then the time derivative of S_3 and S_4 along the system trajectories turns into as follows:

$$\dot{S}_3 = f_3(x) + g_{31}(x)\frac{u_f}{T_0'} - \dot{x}_{3d} = -\alpha_3|S_3|^{\frac{m}{n}}\text{sign}(S_3) - \beta_3|S_3|^{\frac{n}{m}}\text{sign}(S_3) \tag{21}$$

$$\dot{S}_4 = f_4(x) + g_{41}(x)\frac{u_f}{T_0'} + g_{42}(x)\frac{u_q}{T} - \dot{x}_{4d} = -\alpha_4|S_4|^{\frac{m}{n}}\text{sign}(S_4) - \beta_4|S_4|^{\frac{n}{m}}\text{sign}(S_4) \tag{22}$$

where α_3, β_3, α_4 and β_4 are positive design constants.

Therefore, a suitable selection of the control laws (u_f, u_q) to achieve the fixed-time stability is given as follows:

$$\begin{cases} u_f = -\dfrac{T_0'}{g_{31}(x)}\left[f_3(x) - \dot{x}_{3d} + \alpha_3|S_3|^{\frac{m}{n}}\text{sign}(S_3) + \beta_3|S_3|^{\frac{n}{m}}\text{sign}(S_3)\right] \\ u_q = -\dfrac{T}{g_{42}(x)}\left[f_4(x) + g_{41}(x)\dfrac{u_f}{T_0'} - \dot{x}_{4d} + \alpha_4|S_4|^{\frac{m}{n}}\text{sign}(S_4) + \beta_4|S_4|^{\frac{n}{m}}\text{sign}(S_4)\right] \end{cases} \tag{23}$$

where the differentiation of x_{3d} and x_{4d} can be computed by (18) and (19).

Remark 3.1. *The novelty and the difference of this paper compared with existing results are as follows: (i) the development of a fixed-time controller via dynamic surface control method capable of improving transient stability and driving all signals of the over-all closed-loop system to a small neighborhood of the equilibrium point with a fixed time; (ii) the presented control law without directly computing the derivative of virtual control functions at each step; and (iii) the nonlinear first-order filter used instead of linear first-order filter, thereby leading to faster response ability and the shorter settling time to approach the desired equilibrium.*

3.2. **Stability analysis.** The objective of this subsection is to establish that the closed-loop system has the uniformly ultimate boundedness property. First, let us introduce the following error variables:

$$\begin{cases} y_2 = x_{2d} - x_2^* = x_{2d} + \alpha_1|S_1|^{\frac{m}{n}}\text{sign}(S_1) + \beta_1|S_1|^{\frac{n}{m}}\text{sign}(S_1) \\ y_3 = x_{3d} - x_3^* = x_{3d} - P_m + \dfrac{D}{2}x_2 - \dfrac{M}{2}\left(\alpha_2|S_2|^{\frac{m}{n}}\text{sign}(S_2) - \beta_2|S_2|^{\frac{n}{m}}\text{sign}(S_2) - \dot{x}_{2d}\right) \\ y_4 = x_{4d} - x_4^* = x_{4d} + \dfrac{D}{2}x_2 - \dfrac{M}{2}\left(\alpha_2|S_2|^{\frac{m}{n}}\text{sign}(S_2) + \beta_2|S_2|^{\frac{n}{m}}\text{sign}(S_2) - \dot{x}_{2d}\right) \end{cases}$$

Then the derivatives of surface variables and error variables are as follows:

$$\begin{cases} \dot{S}_1 = S_2 + y_2 - \alpha_1|S_1|^{\frac{m}{n}}\text{sign}(S_1) - \beta_1|S_1|^{\frac{n}{m}}\text{sign}(S_1) \\ \dot{S}_2 = -\dfrac{1}{M}(S_3 + S_4 + y_3 + y_4) - \alpha_2|S_2|^{\frac{m}{n}}\text{sign}(S_2) - \beta_2|S_2|^{\frac{n}{m}}\text{sign}(S_2) \\ \dot{S}_3 = -\alpha_3|S_3|^{\frac{m}{n}}\text{sign}(S_3) - \beta_3|S_3|^{\frac{n}{m}}\text{sign}(S_3) \\ \dot{S}_4 = -\alpha_4|S_4|^{\frac{m}{n}}\text{sign}(S_4) - \beta_4|S_4|^{\frac{n}{m}}\text{sign}(S_4) \\ \dot{y}_j = -\dfrac{y_j}{\tau_j} - \dot{x}_j^* \\ \dot{x}_{jd} = -\dfrac{1}{\tau_j}(x_{jd} - x_j^*), \quad j = 2,3,4 \end{cases} \tag{24}$$

To establish the boundedness of the closed-loop system (24), the Lyapunov function candidate is defined as follows:

$$V = \frac{1}{2}\left(\sum_{i=1}^{4} S_i^2 + \sum_{j=2}^{4} y_j^2\right) \tag{25}$$

In order to consider the closed-loop stability analysis of the power systems with STATCOM, the following assumption is made.

Assumption 3.1. *There exists any given positve constant p such that the initial condition satisfies $V(0) = \frac{1}{2}\left(\sum_{i=1}^{4} S_i(0)^2 + \sum_{j=2}^{4} y_j(0)^2\right) \le p$.*

Theorem 3.1. *The power system dynamics with STATCOM (5) are considered. Subsequently, under Assumption 3.1, provided that the following two conditions are such that*

- *The control law is given in (23) where $\alpha_i > 0$, $\beta_i > 0$, $i = 1,2,3,4$,*
- $\alpha_1 = k_{11} + \frac{\lambda_1^{\frac{m}{n}+1}}{\frac{m}{n}+1}$, $\alpha_2 = k_{12} + \frac{\gamma_2^{-(\frac{m}{n}+1)}}{\frac{m}{n}+1} + \frac{2\lambda_2^{\frac{m}{n}+1}}{M(\frac{m}{n}+1)}$, $\alpha_3 = k_{13} + \frac{\gamma_2^{-(\frac{m}{n}+1)}}{M(\frac{m}{n}+1)}$, $\alpha_4 = k_{14} + \frac{\gamma_2^{-(\frac{m}{n}+1)}}{M(\frac{m}{n}+1)}$, $\beta_1 = k_{21} + \frac{\gamma_1^{\frac{n}{m}+1}}{\frac{n}{m}+1}$, $\beta_2 = k_{22} + \frac{2\gamma_2^{\frac{n}{m}+1}}{M(\frac{n}{m}+1)}$, $\beta_3 > 0$, $\beta_4 > 0$, $\frac{1}{\tau_2} > \frac{\eta_2^{\frac{m}{n}+1}}{\frac{m}{n}+1}$, $\frac{1}{\tau_2} > \frac{\lambda_2^{-(\frac{n}{m}+1)}}{\frac{n}{m}+1}$, $\frac{1}{\tau_3} > \frac{\eta_3^{\frac{m}{n}+1}}{\frac{m}{n}+1} + \frac{\lambda_2^{-(\frac{n}{m}+1)}}{M(\frac{n}{m}+1)}$, $\frac{1}{\tau_3} > 0$, $\frac{1}{\tau_4} > \frac{\eta_4^{\frac{m}{n}+1}}{\frac{m}{n}+1}$, $\frac{1}{\tau_4} > \frac{\lambda_2^{-(\frac{n}{m}+1)}}{M(\frac{n}{m}+1)}$ *and* $k_{il} > 0$, $k_{ir} > 0$, $i = 1,2$, $l = 1,2,3,4$, $r = 1,2$ *as given in (29)*

are all satisfied, then all trajectories of the overall closed-loop dynamics (24) are SGFTU-UB.

Proof: Considering the Lyapunov function candidate V as given in (25), then the time derivative of V can be derived as follows:

$$\begin{aligned}\dot{V} = \sum_{i=1}^{4} S_i\dot{S}_i + \sum_{j=2}^{4} y_j\dot{y}_j &= S_1\left(S_2 + y_2 - \alpha_1|S_1|^{\frac{m}{n}}\mathrm{sign}(S_1) - \beta_1|S_1|^{\frac{n}{m}}\mathrm{sign}(S_1)\right)\\ &+ S_2\left(-\frac{1}{M}(S_3+S_4+y_3+y_4) - \alpha_2|S_2|^{\frac{m}{n}}\mathrm{sign}(S_2) - \beta_2|S_2|^{\frac{n}{m}}\mathrm{sign}(S_2)\right)\\ &+ S_3\left(-\alpha_3|S_3|^{\frac{m}{n}}\mathrm{sign}(S_3) - \beta_3|S_3|^{\frac{n}{m}}\mathrm{sign}(S_3)\right)\\ &+ S_4\left(-\alpha_4|S_4|^{\frac{m}{n}}\mathrm{sign}(S_4) - \beta_4|S_4|^{\frac{n}{m}}\mathrm{sign}(S_4)\right)\\ &- \sum_{j=2}^{4} y_j\left(\frac{|y_j|^{\frac{m}{n}+1} + |y_j|^{\frac{n}{m}+1}}{\tau_j} + y_j\dot{x}_j^*\right)\end{aligned} \tag{26}$$

In accordance with Assumption 3.1, there exists a positive constant p such that $\Pi := \left\{\sum_{i=1}^{4} S_i^2 + \sum_{j=2}^{4} y_j^2 \le 2p\right\}$ is a compact set in R^7. Considering the continuous property, the function $\dot{x}_j^*$ has a maximum value B_j for the given initial condition in the compact set Π. According to Lemma 2.2, one has

$$\begin{cases} S_1S_2 \le |S_1||S_2| \le \dfrac{\gamma_1^{\frac{n}{m}+1}}{\frac{n}{m}+1}|S_1|^{\frac{n}{m}+1} + \dfrac{\gamma_1^{-\left(\frac{m}{n}+1\right)}}{\frac{m}{n}+1}|S_2|^{\frac{m}{n}+1}, \quad \gamma_1 > 0\\ S_1y_2 \le |S_1||y_2| \le \dfrac{\lambda_1^{\frac{m}{n}+1}}{\frac{m}{n}+1}|S_1|^{\frac{m}{n}+1} + \dfrac{\lambda_1^{-\left(\frac{n}{m}+1\right)}}{\frac{n}{m}+1}|y_2|^{\frac{n}{m}+1}, \quad \lambda_1 > 0\\ -\dfrac{1}{M}S_2S_l \le \dfrac{1}{M}|S_2||S_l| \le \left[\dfrac{\gamma_2^{\frac{n}{m}+1}}{\frac{n}{m}+1}|S_2|^{\frac{n}{m}+1} + \dfrac{\gamma_2^{-\left(\frac{m}{n}+1\right)}}{\frac{m}{n}+1}|S_l|^{\frac{m}{n}+1}\right], \quad \gamma_2 > 0, \quad l = 3,4\\ -\dfrac{1}{M}S_2y_l \le \dfrac{1}{M}|S_2||y_l| \le \left[\dfrac{\lambda_2^{\frac{m}{n}+1}}{\frac{m}{n}+1}|S_2|^{\frac{m}{n}+1} + \dfrac{\lambda_2^{-\left(\frac{n}{m}+1\right)}}{\frac{n}{m}+1}|y_l|^{\frac{n}{m}+1}\right], \quad \lambda_2 > 0, \quad l = 3,4\\ -y_j\dot{x}_j^* \le |y_j||B_j| \le \dfrac{\eta_j^{\frac{m}{n}+1}}{\frac{m}{n}+1}|y_j|^{\frac{m}{n}+1} + \dfrac{\eta_j^{-\left(\frac{n}{m}+1\right)}}{\frac{n}{m}+1}|B_j|^{\frac{n}{m}+1}, \quad \eta_j > 0, \quad j = 2,3,4 \end{cases} \tag{27}$$

After substituting (27) into (26), we obtain

$$\begin{aligned}\dot{V} = &-\left(\alpha_1 - \frac{\lambda_1^{\frac{m}{n}+1}}{\frac{m}{n}+1}\right)|S_1|^{\frac{m}{n}+1} - \left(\beta_1 - \frac{\gamma_1^{\frac{n}{m}+1}}{\frac{n}{m}+1}\right)|S_1|^{\frac{m}{n}+1}\\ &-\left(\alpha_2 - \frac{\gamma_2^{-\left(\frac{m}{n}+1\right)}}{\frac{m}{n}+1} - \frac{2\lambda_2^{\frac{m}{n}+1}}{M(\frac{m}{n}+1)}\right)|S_2|^{\frac{m}{n}+1} - \left(\beta_2 - \frac{2\gamma_2^{\frac{n}{m}+1}}{M(\frac{n}{m}+1)}\right)|S_2|^{\frac{n}{m}+1}\\ &-\left(\alpha_3 - \frac{\gamma_2^{-\left(\frac{m}{n}+1\right)}}{M(\frac{m}{n}+1)}\right)|S_3|^{\frac{m}{n}+1} - \beta_3|S_3|^{\frac{n}{m}+1} - \left(\alpha_4 - \frac{\gamma_2^{-\left(\frac{m}{n}+1\right)}}{M(\frac{m}{n}+1)}\right)|S_4|^{\frac{m}{n}+1}\\ &-\beta_4|S_4|^{\frac{n}{m}+1} - \left(\frac{1}{\tau_2} - \frac{\eta_2^{\frac{m}{n}+1}}{\frac{m}{n}+1}\right)|y_2|^{\frac{m}{n}+1} - \left(\frac{1}{\tau_2} - \frac{\lambda_2^{-\left(\frac{n}{m}+1\right)}}{\frac{n}{m}+1}\right)|y_2|^{\frac{n}{m}+1}\end{aligned}$$

$$
\begin{aligned}
&-\left(\frac{1}{\tau_3}-\frac{\eta_3^{\frac{m}{n}+1}}{\frac{m}{n}+1}-\frac{\lambda_2^{-\left(\frac{n}{m}+1\right)}}{M(\frac{n}{m}+1)}\right)|y_3|^{\frac{m}{n}+1}-\frac{1}{\tau_3}|y_3|^{\frac{n}{m}+1}-\left(\frac{1}{\tau_4}-\frac{\eta_4^{\frac{m}{n}+1}}{\frac{m}{n}+1}\right)|y_4|^{\frac{m}{n}+1}\\
&-\left(\frac{1}{\tau_4}-\frac{\lambda_2^{-\left(\frac{n}{m}+1\right)}}{M(\frac{n}{m}+1)}\right)|y_4|^{\frac{n}{m}+1}+\sum_{j=2}^{4}\frac{\eta_j^{-\left(\frac{n}{m}+1\right)}}{\frac{n}{m}+1}|B_j|^{\frac{n}{m}+1}
\end{aligned}
\tag{28}
$$

From (28), the suitable design parameters can be chosen as follows:

$$
\begin{cases}
\alpha_1=k_{11}+\dfrac{\lambda_1^{\frac{m}{n}+1}}{\frac{m}{n}+1},\quad \alpha_2=k_{12}+\dfrac{\gamma_2^{-\left(\frac{m}{n}+1\right)}}{\frac{m}{n}+1}+\dfrac{2\lambda_2^{\frac{m}{n}+1}}{M(\frac{m}{n}+1)},\\
\alpha_3=k_{13}+\dfrac{\gamma_2^{-\left(\frac{m}{n}+1\right)}}{M(\frac{m}{n}+1)},\quad \alpha_4=k_{14}+\dfrac{\gamma_2^{-\left(\frac{m}{n}+1\right)}}{M(\frac{m}{n}+1)},\\
\beta_1=k_{21}+\dfrac{\gamma_1^{\frac{n}{m}+1}}{\frac{n}{m}+1},\quad \beta_2=k_{22}+\dfrac{2\gamma_2^{\frac{n}{m}+1}}{M(\frac{n}{m}+1)},\quad \beta_3>0,\quad \beta_4>0,\\
\dfrac{1}{\tau_2}>\dfrac{\eta_2^{\frac{m}{n}+1}}{\frac{m}{n}+1},\quad \dfrac{1}{\tau_2}>\dfrac{\lambda_2^{-\left(\frac{n}{m}+1\right)}}{\frac{n}{m}+1},\quad \dfrac{1}{\tau_3}>\dfrac{\eta_3^{\frac{m}{n}+1}}{\frac{m}{n}+1}+\dfrac{\lambda_2^{-\left(\frac{n}{m}+1\right)}}{M(\frac{n}{m}+1)},\quad \dfrac{1}{\tau_3}>0,\\
\dfrac{1}{\tau_4}>\dfrac{\eta_4^{\frac{m}{n}+1}}{\frac{m}{n}+1},\quad \dfrac{1}{\tau_4}>\dfrac{\lambda_2^{-\left(\frac{n}{m}+1\right)}}{M(\frac{n}{m}+1)}
\end{cases}
\tag{29}
$$

where k_{11}, k_{12}, k_{13}, k_{14}, k_{21}, k_{22} are positive design parameters. Let us define the following parameters:

$$
k_1=\min\{k_{11},k_{12},k_{13},k_{14}\},\quad k_2=\min\{k_{21},k_{13},\beta_3,\beta_4\},\quad k_3=\sum_{j=2}^{4}\frac{\eta_j^{-\left(\frac{n}{m}+1\right)}}{\frac{n}{m}+1}|B_j|^{\frac{n}{m}+1}.
$$

According to Lemmas 2.3 and 2.4, (28) can be rewritten as follows:

$$
\begin{aligned}
\dot V &= -k_1\left(\sum_{i=1}^{4}|S_i|^{\frac{m}{n}+1}+\sum_{j=2}^{4}|y_i|^{\frac{m}{n}+1}\right)-k_2\left(\sum_{i=1}^{4}|S_i|^{\frac{n}{m}+1}+\sum_{j=2}^{4}|y_i|^{\frac{n}{m}+1}\right)+k_3\\
&= -k_1\left(\sum_{i=1}^{4}(S_i^2)^{\frac{\frac{m}{n}+1}{2}}+\sum_{j=2}^{4}(y_j^2)^{\frac{\frac{m}{n}+1}{2}}\right)-k_2\left(\sum_{i=1}^{4}(S_i^2)^{\frac{\frac{n}{m}+1}{2}}+\sum_{j=2}^{4}(y_j^2)^{\frac{\frac{m}{n}+1}{2}}\right)+k_3\\
&\le -7^{\frac{1-\frac{m}{n}}{2}}k_1\left(\sum_{i=1}^{4}S_i^2+\sum_{j=2}^{4}y_j^2\right)^{\frac{\frac{m}{n}+1}{2}}-k_2\left(\sum_{i=1}^{4}S_i^2+\sum_{j=2}^{4}y_j^2\right)^{\frac{\frac{n}{m}+1}{2}}+k_3\\
&= -2^{\frac{\frac{m}{n}+1}{2}}7^{\frac{1-\frac{m}{n}}{2}}k_1V^{\frac{\frac{m}{n}+1}{2}}-2^{\frac{\frac{n}{m}+1}{2}}k_2V^{\frac{\frac{n}{m}+1}{2}}+k_3
\end{aligned}
\tag{30}
$$

The designed parameters are able to be suitably chosen such that $-2^{\frac{\frac{m}{n}+1}{2}}7^{\frac{1-\frac{m}{n}}{2}}k_1V^{\frac{\frac{m}{n}+1}{2}}-2^{\frac{\frac{n}{m}+1}{2}}k_2V^{\frac{\frac{n}{m}+1}{2}}+k_3\le 0$ holds. In accordance with Assumption 3.1, it is easy to obtain $\dot V\le 0$. Thus, $\Omega:=\{V\le p\}$ is an invariant set. It means that if $V(0)\le p$, then for all $t\ge 0$, one has $V(t)\le p$. For the ultimate bound of the closed-loop dynamics, we can solve it from the following equation:

$$
-2^{\frac{\frac{m}{n}+1}{2}}7^{\frac{1-\frac{m}{n}}{2}}k_1V^{\frac{\frac{m}{n}+1}{2}}-2^{\frac{\frac{n}{m}+1}{2}}k_2V^{\frac{\frac{n}{m}+1}{2}}+k_3=0
\tag{31}
$$

It is clear that the expression above is a polynomial algebraic equation with fractional exponent. Thus, it is rather difficult to find an analytical solution for the equation above. Nevertheless, we need to compute a rough estimation for the ultimate bound of the closed-loop dynamics from the following two equations:

$$-2^{\frac{\frac{m}{n}+1}{2}}7^{\frac{1-\frac{m}{n}}{2}}k_1V^{\frac{\frac{m}{n}+1}{2}}+k_3=0,\quad -2^{\frac{\frac{n}{m}+1}{2}}k_2V^{\frac{\frac{n}{m}+1}{2}}+k_3=0.$$

After computing two equations above, one has the following ultimate bound of the closed-loop dynamics:

$$\lim_{t\to+\infty}V(t)\le 2\min\left\{\frac{k_3}{\left(2^{\frac{\frac{m}{n}+1}{2}}7^{\frac{1-\frac{m}{n}}{2}}\right)^{\frac{2n}{n+m}}},\frac{k_3}{\left(2^{\frac{\frac{n}{m}+1}{2}}k_2\right)^{\frac{2m}{m+n}}}\right\}\le V(0)\le p \tag{32}$$

Therefore, all signals of the closed-loop system, i.e., S_i and y_j, are SGFTUUB. Further, x_i and x_j^* are SGFTUUB.

From Lemma 2.1, it is easy to obtain $\bar{\alpha}=2^{\frac{\frac{m}{n}+1}{2}}7^{\frac{1-\frac{m}{n}}{2}}k_1$, $\bar{\beta}=2^{\frac{\frac{n}{m}+1}{2}}k_2$, $\varsigma=k_3$, $\bar{m}=\frac{m}{n}+1$, $\bar{n}=2$, $\bar{p}=\frac{n}{m}+1$, $\bar{q}=2$. Moreover, the closed-loop dynamics can be stablized in the arbitrarily small neighborhood of the origin by selecting suitably control parameters. According to Lemma 2.1 the converge time is bounded by

$$T_f\le T_{\max}=\frac{1}{2^{\frac{\frac{m}{n}+1}{2}}\times 7^{\frac{1-\frac{m}{n}}{2}}k_1}\cdot\frac{n}{\frac{m-n}{2}}+\frac{1}{2^{\frac{\frac{n}{m}+1}{2}}k_2\left(2^{\frac{m+n}{2m}}-1\right)}\cdot\frac{m}{\frac{m-n}{2}} \tag{33}$$

This completes the proof.

4. **Simulation Results.** In this section, in order to verify the effectiveness of the proposed nonlinear controller. The proposed controller is evaluated via simulations on a Single-Machine Infinite Bus (SMIB) power system including STATCOM as shown in Figure 1. The performance of the proposed control scheme is evaluated in MATLAB environment.

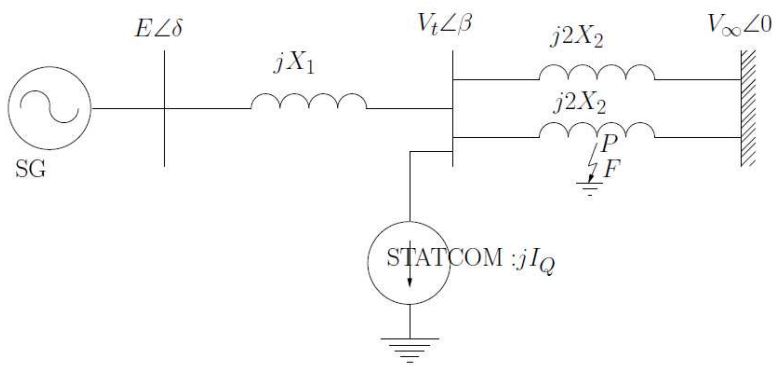

FIGURE 1. A single line diagram of SMIB model with STATCOM

The physical parameters (pu.), the controller parameters, and initial parameters used for this power system model are as follows.

- The parameters of synchronous generators, STATCOM, and transmission line: $\omega_s=2\pi f$ rad/s, $D=0.2$, $H=5$, $f=60$ Hz, $T_0'=4$, $V_\infty=1\angle 0°$, $X_d=1.1$, $X_d'=0.2$, $X_T=0.1$, $T=1$, $X_2=X_L=0.2$, $P_m=1$.

- The control parameters of the proposed controller are $c_i = 20$, $(i = 1, 2, 3, 4)$, $\tau_j = 0.01$, $m = q = 4$, $n = p = 3$.
- Initial parameters $\delta_e = 0.4964$ rad, $\omega_e = \omega_s$, $P_{ee} = 1$ pu., $P_{se} = 0$ pu.

The time domain simulations are carried out to evaluate the presented control law, as given in (23), for the stability enhancement and improved transient performances. The performance of the proposed nonlinear controller (fixed-time dynamic surface control) is compared with that of the Conventional Dynamic Surface Control (CDSC) (34) as follows:

$$\begin{cases} u_{fdsc} = -\dfrac{T_0'}{g_{31}(x)}\left[f_3(x) - \dot{x}_{3d} + c_3 S_3\right] \\ u_{qdsc} = -\dfrac{T}{g_{42}(x)}\left[f_4(x) + g_{41}(x)\dfrac{u_f}{T_0'} - \dot{x}_{4d} + c_4 S_4\right] \end{cases} \tag{34}$$

where $S_1 = x_2$, $S_j = x_j - x_j^*$, $x_2^* = -c_1 S_1$, $x_3^* = P_m - \frac{Dx_2}{2} + \frac{M}{2}(c_2 S_2 + \dot{x}_{2d})$, $x_4^* = x_3^* - P_m$, $\dot{x}_{jd} = -\frac{1}{\tau_j}\left(x_{jd} - x_j^*\right)$. The controller parameters of this scheme are set as $c_i = 20$, $(k = 1, 2, 3, 4)$, $\tau_j = 0.01$.

For the simulations, there are two cases used to evaluate the performance of the developed controller. One is a symmetrical three phase short circuit occurring on one of the transmission lines as shown in Figure 1. The other is a small perturbation to mechanical power to synchronous generators in the system. The two cases of interest are as follows.

Case 1: Effect of severe disturbance

Assume that there is a three-phase fault occurring at the point P as shown in Figure 1. For this case, we assume that there are five stages of interest as follows. Firstly, all state variables are at pre-fault steady state. The fault occurs at $t = 0.5$ sec. After that, the fault is isolated by opening the breaker at $t = 0.7$ sec. The transmission line can be restored at $t = 1.5$ sec. Eventually, the system returns to a post-fault state.

Case 2: Effect of small disturbance due to small perturbation in mechanical power

For this case, we assume that there are three stages of interest as follows. First, the system is in a pre-fault steady state. Subsequently, there is a 30% increase in the mechanical power between $t = 0.5$ sec. and $t = 1.5$ sec. After that, the system is in a post-fault state.

The simulation results are shown in Figures 2 and 3 and discussed as follows. It is observed from Case 1 that Figure 2 is obtained to exhibit the time responses of power angle (δ), frequency ($\omega - \omega_s$), transient voltage (E) and STATCOM current (I_Q), respectively. From using the presented and CDSC schemes, all time responses converge to the pre-fault state values in fixed time. Figure 3 shows the active power ($P_e + P_s$) and terminal voltage (V_t) under the proposed control and the CDSC methods. It is also observed that the developed method provides obviously faster convergence rate compared with the CDSC, and its settling time function can be found from control parameters. Moreover, the proposed strategy can rapidly suppress power oscillations once compared with the results from the CDSC scheme in fixed-time. These confirm clearly that the presented control law accomplishes transient stability improvement together with frequency and voltage regulation. Additionally, this shows the superior performance of the proposed control strategy.

Similarly, for Case 2, under the effect of a 30% perturbation ($\Delta P_m = 0.3P_m$) of mechanical input power, the time responses of power angle, frequency, active power, and terminal voltage are shown in Figures 4 and 5. They obviously exhibit the tracking performance superiority of the proposed over the CDSC method in fixed time. From figures, it can be seen that all time trajectories rapidly reach a steady-state condition, thereby

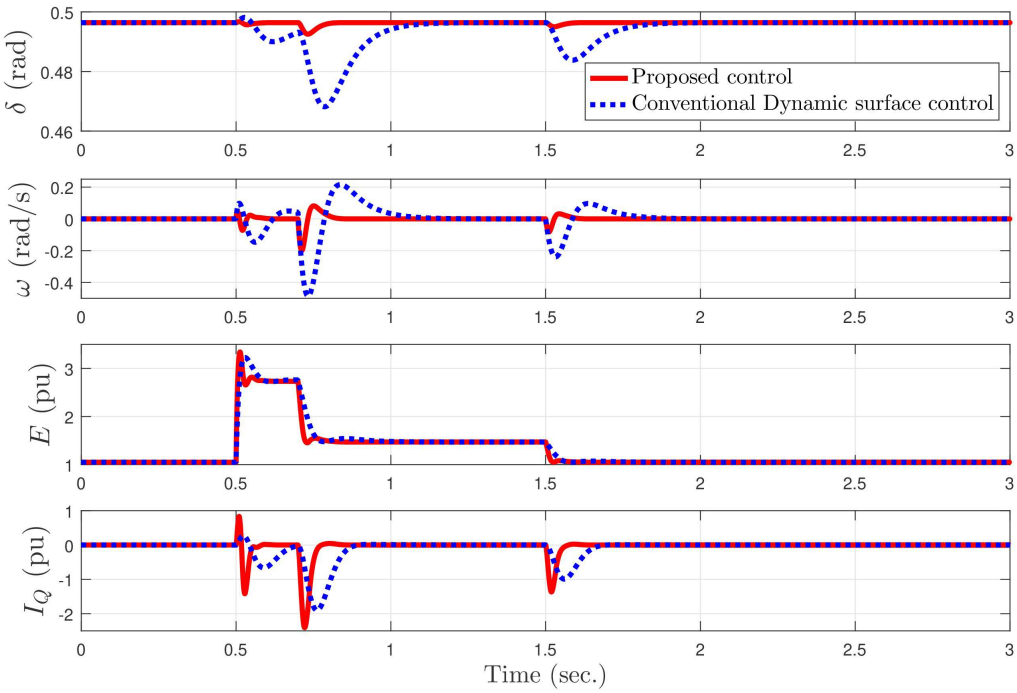

FIGURE 2. Case 1: Controller performance – Power angles (δ) (rad.), frequency ($\omega - \omega_s$) rad/s, transient voltage E, and STATCOM current I_Q (Solid: Proposed control, Dashed: Dynamic surface control)

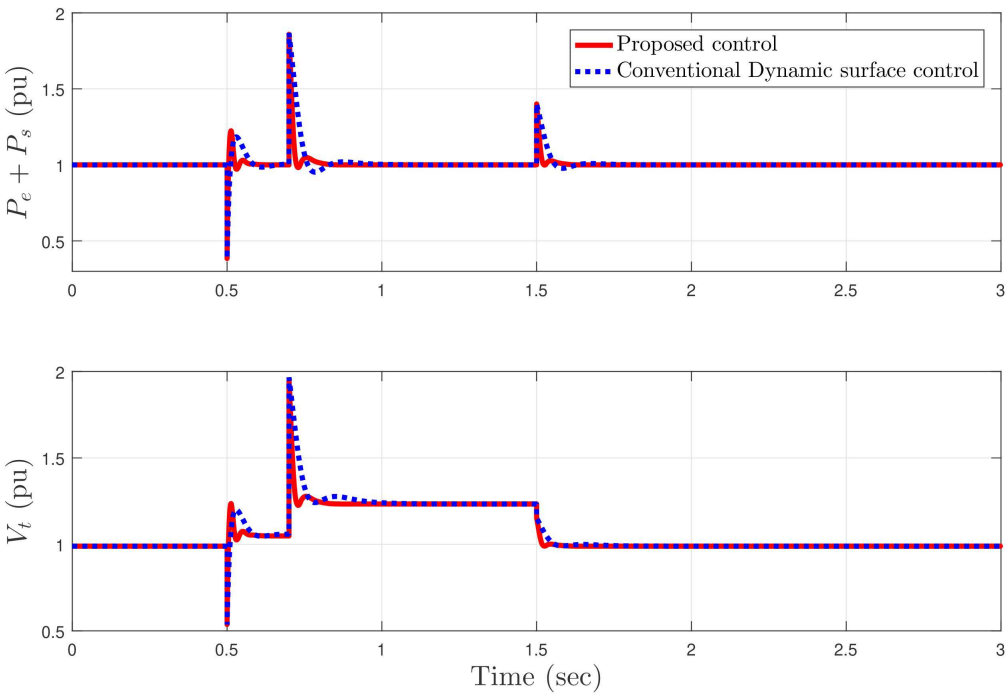

FIGURE 3. Case 1: Controller performance – Active power ($P_e + P_s$) (pu.) and the terminal voltage (V_t) (pu.) (Solid: Proposed control, Dashed: Dynamic surface control)

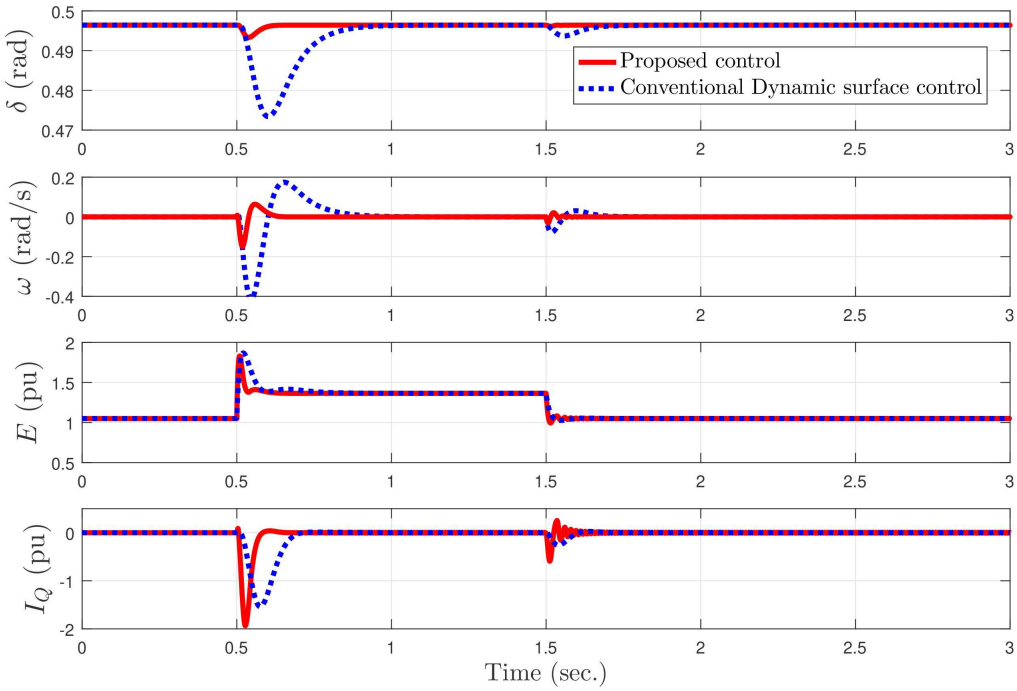

FIGURE 4. Case 2: Controller performance – Power angles (δ) (rad.), frequency ($\omega - \omega_s$) rad/s, transient voltage E, and STATCOM current I_Q (Solid: Proposed control, Dashed: Dynamic surface control)

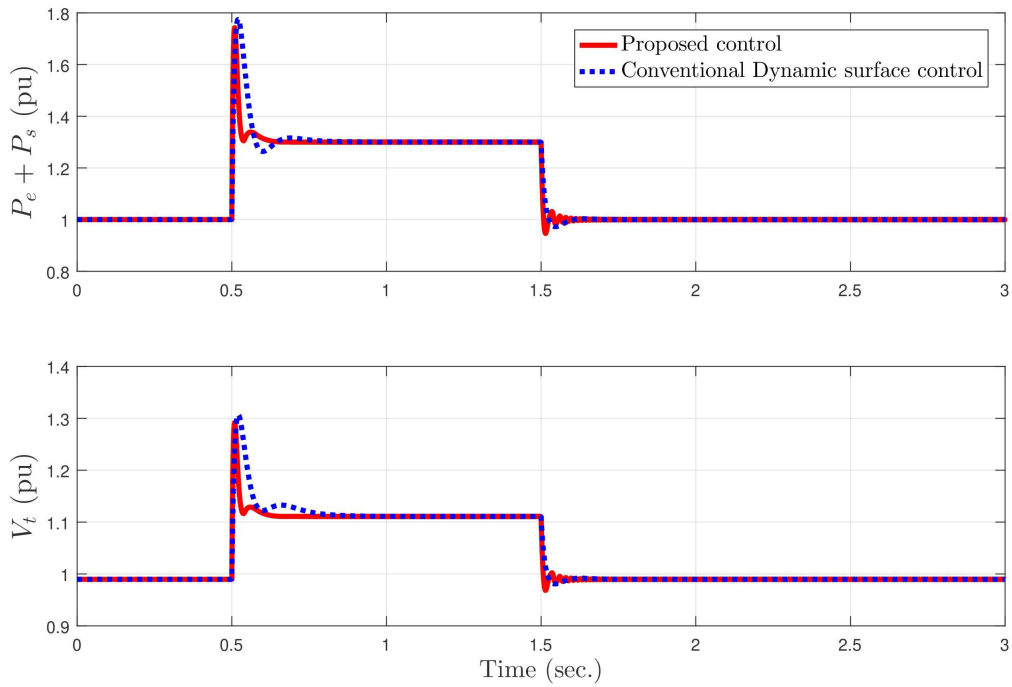

FIGURE 5. Case 2: Controller performance – Active power ($P_e + P_s$) (pu.) and the terminal voltage (V_t) (pu.) (Solid: Proposed control, Dashed: Dynamic surface control)

exhibiting the closed-loop system stability in fixed-time. Additionally, the time responses of the presented controller are less oscillatory than the time responses given by the CDSC. Therefore, the developed control provides significantly better damping enhancement in the power oscillation. Further, it is easy to observe that the rise time and settling time are obviously decreased.

From the simulation results with two different cases, from (33), the fixed time can be directly computed from the design parameters to obtain: $T_{\max} = \frac{6}{k_1 2^{7/6} 7^{-1/7}} + \frac{8}{k_2 2^{7/8}(2^{7/8}-1)}$. According to the second condition of Theorem 3.1, provided that we select $k_1 = k_2 = 1$, the fixed time becomes $T_{\max} = 10.3429$ sec. From Figures 2-5, after the system is disturbed, all system states converge to the desired equilibrium within 0.16 sec., which is less than the upper bound $T_{\max} = 10.3429$ sec. Therefore, it is obvious to conclude that the proposed control law can be applied for transient stabilization and voltage regulation following small and large disturbances in fixed time. The developed control strategy can make the closed-loop dynamic behaviors of the system converge quickly into a neighborhood of the desired equilibrium point. Meanwhile, the time responses of all trajectories return rapidly to the steady-state value condition after the fault is cleared or the small disturbance vanishes. Further, the fixed-time control method stabilizes the closed-loop system faster than the CDSC method does. In particular, it obviously outperforms the CDSC scheme in terms of faster response ability and damping enhancement in the power oscillation in a shorter settling time.

Practically, an accurate model of the power system is often unavailable. In particular, there are unavoidable parameter variations in the system. As a result, the robustness evaluation of the developed scheme is of great importance. It is well-known that many parameters of the power system can be uncertain, i.e., the inertial constant H and the

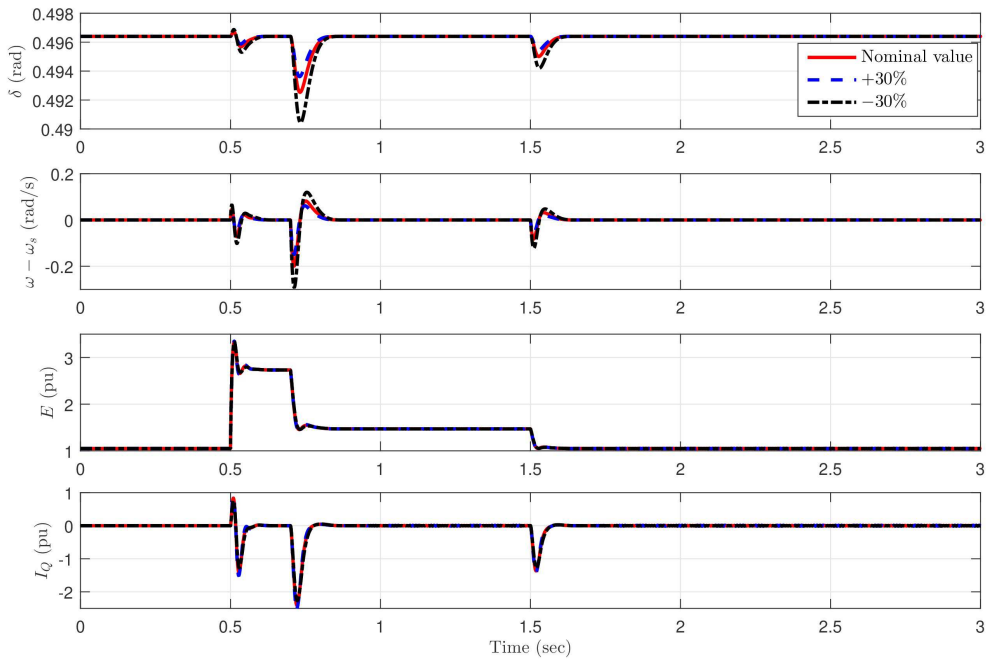

FIGURE 6. Time histories of power angles (δ) (rad.), frequency ($\omega - \omega_s$) rad/s, transient voltage E, and STATCOM current I_Q under parameter variations of the inertial constant H (Solid: nominal value, Dashed: +30%, Dashdotted: −30%)

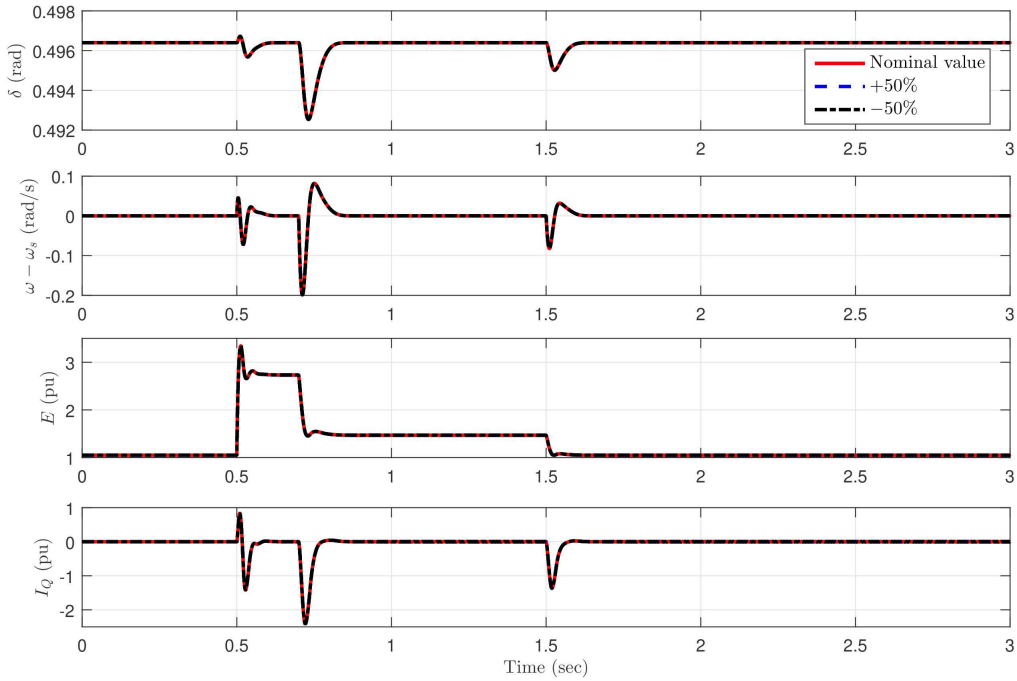

FIGURE 7. Time histories of power angles (δ) (rad.), frequency ($\omega - \omega_s$) rad/s, transient voltage E, and STATCOM current I_Q under parameter variations of time constant T_0' (Solid: nominal value, Dashed: +50%, Dash-dotted: −50%)

time constant T_0'. It is also difficult to estimate precisely these parameters. Consequently, it is necessary to evaluate the robustness of the proposed control law over these variations.

A robustness test has been carried out by considering a changing of two generator parameters from their nominal values, i.e., the inertial constant H and the time constant T_0' of Case 1. In particular, a ±30% of variation in the value of H as well as a ±50% of variation in the value of T_0' is taken into account for this test. In comparison with the system responses under normal conditions, it is observed from Figures 6 and 7 that the developed method can still offer consistent control performance although there are variations in system parameters. Thus, it can be concluded that the resulting controller is not sensitive to parameter variations.

5. **Conclusions.** In this paper, a fixed-time control scheme has been developed for power systems including STATCOM. To avoid the problem of "explosion of complexity" arising in computing the derivative of the virtual control functions, the proposed method has been developed by a combined fixed-time control and dynamic surface design. Based on this approach, it makes system dynamic performances further improved as compared with the conventional dynamic surface control. Based on Lyapunov control theory, the overall closed-loop stability analysis has been shown to ensure that all trajectories are semi-globally fixed-timely uniformly ultimately bounded. The simulation results have confirmed the efficiency and superiority of the proposed method capable of improving obviously faster transient performances than the conventional dynamic surface method. Extension of this scheme of this paper into a nonlinear fixed-time dynamic surface control for multi-machine power systems with STATCOM in the presence of unknown parameters,

other kinds of FACTS devices, or hybrid power generation (renewable energy) [22] is our future direction.

REFERENCES

[1] P. Kundur, *Power System Stability and Control*, McGraw-Hill, 1994.

[2] A. Kanchanahanathai, V. Chankong and K. A. Loparo, Nonlinear generator excitation and superconducting magnetic energy storage control for transient stability enhancement via immersion and invariance, *Transactions of the Institute of Measurement and Control*, vol.37, no.10, pp.1217-1231, 2015.

[3] N. G. Hingorani and L. Gyugyi, *Understanding FACTS: Concepts and Technology of Flexible AC Transmission Systems*, IEEE Press, 1999.

[4] Y. H. Song and A. T. John, *Flexible AC Transmission Systems (FACTS)*, IEE Power and Energy Series 30, London, U.K., 1999.

[5] L. Gu and J. Wang, Nonlinear coordinated control design of excitation and STATCOM of power systems, *Electric Power System Research*, vol.77, no.7, pp.788-796, 2007.

[6] A. Kanchanahanathai, Nonlinear adaptive controller design for power systems with STATCOM via immersion and invariance, *ECTI Trans. Electrical Engineering, Electronics, and Communications*, vol.14, no.2, pp.35-46, 2016.

[7] Q. J. Liu, Y. Z. Sun, T. L. Shen and Y. N. Song, Adaptive nonlinear co-ordinated excitation and STATCOM based on hamiltonian structure for multimachine-power-system stability enhancement, *IEE Proc. of Control Theory and Applications*, vol.150, no.3, pp.285-294, 2003.

[8] K. Wang and M. L. Crow, Hamiltonian theory based coordinated nonlinear control of generator excitation and STATCOMs, *Proc. of North American Power Symposium*, 2010.

[9] B. Zou and J. Wang, Coordinated control for STATCOM and generator excitation based on passivity and backstepping technique, *Proc. of Electric Information and Control Engineering*, 2010.

[10] A. Kanchanahanuthai, V. Chankong and K. A. Loparo, Transient stability and voltage regulation in multi-machine power systems vis-*à*-vis STATCOM and battery energy storage, *IEEE Trans. Power Systems*, vol.30, no.5, pp.2404-2416, 2015.

[11] A. Kanchanaharuthai, Immersion and invariance-based non-linear coordinated control for generator excitation and static synchronous compensator for power systems, *Electric Power Components and Systems*, vol.42, no.10, pp.1004-1015, 2014.

[12] A. H. Abolmasoumi and M. Moradi, Nonlinear T-S fuzzy stabilizer design for power systems including random loads and static synchronous compensator, *International Trans. Electrical Energy Systems*, vol.28, no.1, pp.1-19, 2018.

[13] A. Kanchanaharuthai and E. Mujjalinvimut, A nonlinear controller for power system with STATCOM based on backstepping and rapid-convergent differentiator, *International Journal of Innovative Computing, Information and Control*, vol.15, no.3, pp.1079-1091, 2019.

[14] M. Krstic, I. Kanellakopoulos and P. V. Kokotivic, *Nonlinear and Adaptive Control Design*, John Willey & Sons, 1995.

[15] J. Ni, L. Lin, C. Liu, X. Hu and T. Shen, Fixed-time dynamic surface high-order sliding mode control for chaotic oscillation in power system, *Nonlinear Dynamics*, vol.86, pp.401-420, 2016.

[16] D. Swaroop, J. K. Hedrick, P. P. Yip and J. C. Gerdes, Dynamic surface control for a class of nonlinear systems, *IEEE Trans. Automatic Control*, vol.45, no.10, pp.1893-1899, 2000.

[17] J. A. Farrell, M. Polycarpou, M. Sharma and W. Dong, Command filtered backstepping, *IEEE Trans. Automatic Control*, vol.54, no.6, pp.1391-1395, 2009.

[18] A. Levant, Higher-order sliding modes, differentiatation and output-feedback control, *International Journal of Control*, vol.76, nos.9-10, pp.924-941, 2003.

[19] G. Hardy, J. Littlewood and G. Polya, *Inequalities*, Cambridge University Press, London, 1951.

[20] Z. Y. Zuo and L. Tie, A new class of finite-time nonlinear consensus protocols for multi-agent systems, *International Journal of Control*, vol.87, no.2, pp.363-370, 2014.

[21] X. Xie, N. Duan and C. Zhao, A combined homogeneous domination and sign function approach to output-feedback stabilization of stochastic high-order nonlinear systems, *IEEE Trans. Automatic Control*, vol.59, no.5, pp.1303-1309, 2014.

[22] S. H. Ahsan, S. Manjang, M. Baharuddin and Syafaruddin, Real-time performance model of hybrid power generation (landfill gas, photovoltaic system, diesel generator), *ICIC Express Letters*, vol.13, no.6, pp.435-444, 2019.